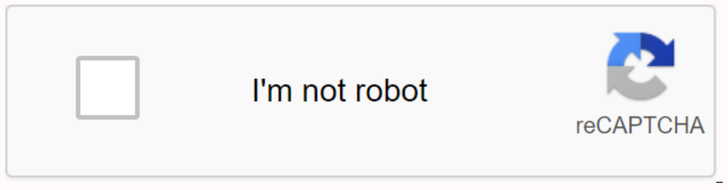


Continue

# World of tanks memes

The level of Fermi is the same for both metal and semiconductor elements, and semiconductor conductivity in a region close to the surface is no different from its conductivity volume. From: Cilika Acta Analyst, 2006 Ohtani, in Advances in Inorganic Chemistry, 2011Fermi level is a kind of measure of equilibrium electronic energy of solid material. It is believed that the level of Fermi is located just below the bottom of the CB and above the upper VB for n-type and p-type semiconductor materials (13), respectively. Most metal oxides are categorized as n-type semiconductors with farm levels more catode (higher) than the standard electrode potential of electrolysis in contact with metaloxide and thus electrons in donor levels just below CB are injected into the electrolyte to form the layer of space (depletion) with an electric field, i.e. Schottky barrier. In the 1980s, this internal electrical field was thought to be effectively divided into e-h + ; i.e. e- and h+ migrate to bulk and surfaces of semiconductor electrodes and particles, but this does not appear to be the case for untreated photocatalist particles due to the expected large thickness of this layer due to very low donor density levels in ordinary photocatalist particles. Norio Sate, in electrochemistry in metal and semiconductor electrodes, 1998As the level of Farms of the electrode approaches the surface level of a high degree of density, the surface condition is charged or diluted as a capacitor. For convenience, we express the sum of σss and σd in Eqn. 5-86 as a charge surface state Qss and the capacity due to the surface condition charge as surface state capacity Css. Then, the interphase capacity C is represented by the capacity of the equivalent scheme shown in Fig. 3. Equivalent contour for a two-layer interphase electrolayer comprising a layer for the accumulation of space, surface state and compact layer in semiconductor electrodes: CSC = capacity of a layer for accumulating space; CSS = surface state capacity; CH = compact layer capacity; Rss = load resistance and surface status unloading. The surface capacity of the condition, Css, is apparently zero in the potential range, where the level of Farms is located far from the surface level (the state of the strip edge level). As the fermi level is pinned to the surface, the CSS capacity increases to the maximum, which is equivalent to the CH capacity of the compact layer, since charging the surface condition is equivalent to the compact charging of the layers in the state of the foetal spinning. We think it's now a dropped layer for a cosmic charge that is gradually polarizing in the anodical direction. While the farm level is located far from the surface condition, the interphase capacity is determined by the capacity of the which is subject to a mott-shot connection as shown in Fig. 13. Fig. Mott-Schottky plot of n-type semiconductor electrode in the presence of surface state: Efb = potential with flat range with surface state completely free positive charge; Efb = potential of the flat strip with a superficial state, fully occupied by a positive charge; QSS = maximum surface status charging; εss = surface state level, C = surface status capacity (≒CH). As the fermi level reaches the surface status level, the interphase capacity is determined by the compact layer capacity (maximum surface capacity) and remains constant in a range of potential where farm level is hooked. The further increase in anodical polarization leads again to the capacity of the depletion layer in accordance with another mott-shot plot parallel to the previous plot, as shown in Fig. 3. The equal potential obtained by the Mott-Schottky plot changes in the anodical direction as a result of the anodical charging of the surface condition. This change in the potential of the flat band is equal to the change in the potential of the compact layer, δΔφH (Qss/CSS = Qss/CH), due to the anodical charging of the state of the surface.J. Robertson, in Complex Semiconductor Science and Technology, 2011There are two questions. First, what causes the farm level when observed, and secondly, what is now the state of migs model. Fermi-level metal is thought to be an external effect due to oxygen jobs and strip bending in oxide (Akasaka, etc., 2006; 2006; Robertson et al., 2007; (2004, 2004). Jobs are created only by high temperature heating. O the free position is neutral and creates an energy level in the oxide near Si CB energy occupied by two electrons (Xiong et al., 2005). These electrons can obtain energy by lowering themselves to the level of the Metal Farms as shown in Figure 53. The energy of the formation of neutral oxygen free space is large (Broqvist and Pasquarello, 2006) when it comes to the molecule O2, 6.3 eV of o atom. Thus, the equilibrium concentration of O vacancies in bulk HfO2 is expected to be very small. The formation of the charged free space is reduced by dropping the electrons to the metal (Figure 53(b)), but not much. 53. Charging scheme transfer from the vacancy to a metal electrode for hooking electronegative (pFET) metals, and the group bends. Demkov (2006) noted that that the energy for the formation of vacancies is reduced if the released O reacts with the metal gate to form metal oxide in the metal: (18)OO+(1/n)M=VO2++(1/n)MOn+2e−In the case of Mo, this gives an energy increase of 3,1 eV per O. This reduces the formation energy to about 1,7 eV. However, this is still not enough to create a high concentration of vacancies needed to bend the tape. The relative importance of the oxygen reaction with the metal gate can be seen display of the bulk-free energy of oxide MOn of O relative to the working function of the metal as shown in Figure 54. Reactive metals have low operating functions and large (negative) non-effusive energies. There is a rough linear dependence until the trend is saturation for metals more reactive than Hf.Figure 54. Free energy to form bulk oxides of o atom against metal function. The reaction appears the mechanism of Akasaka et al. (2006), which is shown schematically in Figure 55 (for simplicity, we put all available places at a total distance from the metal). After creating O, O reacts with Si from the channel or in the interphacial layer to create a unit of SiO2,(19)OO+Si=VO2++1/2SiO2+2e−Figure 55. Scheme of charge transfer and oxygen reaction for one metal- HfO2-silicon stack. The electrons at the site are still falling at the level of the Metal Farms, gaining energy. The creation of 1/2SiO2 (instead of saying MoO2) wins 4.7 eV, a large amount, and this significantly reduces the formation of the vacancy (Robertson et al., 2007). The reduction is sufficient that for metals with operating functions above 5.2 eV, the calculated energy of the formation becomes negative. Thus, before bending the strips, the concentration of vacancies will be high. Loaded vacancies lead to bending of the stripes, which raises the stripes in the metal in relation to the oxide, which lowers the EWF metal. The group, which bends in oxide, retreats from the energy pressure from the electrons that fall to the level of the metal Fermi, further changing their composition (Figure 55). It should be noted that this simple model does not include a number of small errors, such as the effects of image loading and differences in calculated oxide formation energies and energy to form vacancies, but in general the model has the right chemical trends. This model is consistent with the observations of Cartier and others. The attachment occurs above 600 °C, as O must be diffused to react with Si. The increased thickness of the SiO2 interphasy layer counteracts diffusion and stops the effect. Hooking can be reversed by O saturation if vacancies can be filled with oxygen (Cartier et al., 2009). External fixator farms is most noticeable for p-metal in smaller piles of EOT. This is known as the lethal effect (Lee et al., 2006) as shown in Figure 46(b). (2007), Akiyama et al. (2008), and Schaeffer et al. (2007a) have produced models to explain this effect based on oxygen transfer.S. Zhao, Z. Mi, in semiconductors and semimetals, 2017Long-level Farms in nanovises was studied by XPS experiments (Zhao et al., 2013b). Illustration in Fig. 13. 13, mg-jerking InN with a wide range of doping concentrations Mg showed no accumulation of surface electron, fermi level near the surface is located near or below the conductivity conductivity of the an edge that is unlike the presence of surface accumulation of electron from mg-opol-ndated epilers (Ager et al., 2008; Anderson et al., 2006; 2007 and 2011). Another very important feature observed by Fig. 13. For example, InN n newspapers with the highest Mg doping concentration studied in this study (with an mg cell temperature of 240°C) indicate a near surface Fermi level of ~ 0.15 eV above VBM.Fig. XPS spectrum of mg-celled InN nanoshirs with different Mg doping concentrations. The panels (A) – (E) correspond to mg cell temperatures of 190, 210, 220, 230 and 240° C respectively (higher mg cell temperature, higher doping mg concentration) (Zhao et al., 2013b). First in principle calculations were carried out further to understand Mg doping in the InN nanomalet (Zhao et al., 2013b). It was found that in the substitution mg dopant there is significantly lower energy to form the surface compared to that in the bulk area, subsequently leading to preferential inclusion of Mg dopant in the region on a nearby surface. However, direct doping of Mg in InN nanosothers suffers significantly from the large surface desorption of Mg at high growth temperatures. This largely explains the almost articulated surface measured by inN nanomuika with relatively low concentrations of doping Mg, for example, samples with mg cell temperatures below 220 ° C, shown in Fig. 3. Since the increase in the concentration of Mg doping, Mg surface embedding dominates the Surface Desorption of Mg, which leads to the achievement of p-type surface.S.B. ... J.C. , in theoretical and computational chemistry, 2004Band crossing the farm level is also supposed to be an essential physics of static quantum size effects (SQSE) in metal UTFs. Here the control parameter is UTF thickness, not compression, since in the transient metal L Were discussed. JCB and SBT are published widely on this issue, so we only summarize some of the most interesting features here. Jellium models [104] predict thickness-dependent oscillations in the operating function φ caused by new bands touching the farm level, with the thickness increasing. Our calculations [90] of Li 1-5Ls showed only weak evidence of oscillations. Note that in passing, that the surface energies in this paper are incorrect; [ref. 20], [21]. However, we found a very strong SQSE in NE(sF), the density of countries at farm level. This is a direct consequence of two-dimensional periodicity. In the jelly pattern 2D periodic system there is a step in ne at the edge of the tape. Although these UTF are far from free electron in many ways (as well as metal, contrary to conventional wisdom [105], the density of states adds one step per layer, which makes SQSE. SQSE was found in a study of hexagonal Al 1-7Ls [107]. By virtue of large bases and tight scanning of the Brillouin zone, we found that φ for 1L to 7L was 4.873 eV, 4.636 eV, 4.372 eV, 4.323 eV, 4.553 eV, and 4.482 eV. Thus, there was a decrease for ν = 1 → 4, a jump for ν = 5, followed by another drop. Essentially, the same behaviour is detected with energy on the surface, except that the minimum value is for ν = 3 and the saturation appears to be set by ν = 7.In Nanostructured semiconductor oxides for the next generation of electronics and functional devices, 2014 Fermi level position determines the concentration of the carrier charge (the carrier charge is free electrons and holes) and the extent to which defects in the semi-product have been ionized. This depends on two important factors: 18,27,291.the nature and concentration of the mixture in the semiconductor; These two factors make the level of farms move across the energy spectrum. The introduction of impurities of the donor shifts the level of Farms upwards, while the introduction of the intake of the impurity moves it downwards. Typically, the level of Fermi is located by the electrical neutrality of the crystal or, if the crystal is charged, by storing the charge. Let's find the position at farm level for a neutral semiconductor with a kind of donor as an admix. We mean with n and p, just as we did in the previous sections, the concentration of electrons in the conductivity and concentration of holes in the valence group, while X0 and X+ will be considered as the concentrations of neutral and charged donors. The state of electrical neutrality is simply thatIt means that n ≥ p and, therefore, EF ≥ Ei. According to (1.60) and (1.61) where ED is donor level [we assume that ED > (Ec + Ev)/2; see Fig. Substitute (1.63) and (1.55) in (1.63), we get the third equation for exp[(EC - EF)/kT] or exp[(EF - Ev)/kT]. There are three cases for which we can easily solve this equation: 1.When the temperature is low enough, so that THE TEX-EF-EvkT<exp-EF-EDkT<1(1.62) gives and therefore, replacement of (1.64) c (1.55) givesIt is clearly visible that at T = 0 the fermi level is in the middle of the forbidden gap between conductivity and donor levels and, as the temperature rises, The level of Farms changes, and the greater the X is, the slower it moves.2.When the temperature is intermediate, sonpXexp−EF-EvkT<1<exp-EF-EDkTEq. (1.62) yields, and therefore a replacement of (1.64) in (1.55) yieldsCan be seen that in this case the concentration of free electron is temperature independent, and the level of Farms turns out to be below donor levels and continues to move downwards as the temperature rises.3.When the temperature is high, soNpExp-EF-EvkT<exp−EF-EDkT(1.62) semiconductor crystal becomes semiconductor i -type [see (1.58) and (1.59)]. After (1.64), (1.66) and (1.68) we can describe the ef temperature dependency on the assumption that Np = Nn (see Fig. 1.9a). On Fig. 13, 201 The different curves of Figure 1.9a and 1.9b correspond to different X values (the figures indicate an increase in X).1.9. Temperature dependence of the position of the farm level and the concentration of electrons for semiconductor elements: (a) Np = Nn; (b) in n relation to dependence on 1/T. Colin Boxall, in complete chemical kinetics, 1999That energy of Fermi or Farm level, Eff, of solid is that energy, where the probability of filling the level of the electronic energy level is exactly 0.5. Chemically, the energy of the farms corresponds to the electrochemical potential of the electrons in the solid. In equilibrium, all electronically conductive materials in contact have the same energy of Fermi. It can be demonstrated that Fermi's energy of an electrolyte containing a pair of redox is equal to the energy level of Nernst associated with the redox pair [95, 125], i.e. for the total pair of reducto-related energy Nernst is associated with the fermi energy electrolyte, Ef, el, from:(9.9)E(Ox/Red)=Ef=ef=q(EOx/Red0+RTnFln(aOxaRed)+C,where C is the difference between this electrochemical scale and the physical vacuum scale and all other symbols have their meaning. Thus, the need for spontaneous electron transfer from solid to reducing active appearance in electrolyte is turned over for spontaneous transfer of electron from electrolyte to solid electrolyte. , the location of Ferma's energy is given by one of the following expressions: (9.11a)Ef=ECB+ kTln (nNCB), (9.11b) Ef=EVB-kTln(pNVB), where the ECB, NCBs and n are the conductivity of edge energy, the density of states in the conductivity and density of electrons in conductivity respectively, and EVB, NVB and p are the corresponding quantities for holes in the valent range. Thus, from equations (9.11) it can be seen that in the dark, for semiconductors of n-type, Eff is located very close to the ECB, and for an inherent semiconductor, Eff is located in the center of the gap of the tape. Regardless of the type of semiconductors, the condition described in the equation (9.10) still holds spontaneous electronic transmission between an electrolyte containing an active bioactive species and a semiconductor in the dark. In order to make Nernst's electrolyte energies comparable to the energies of the chargers in the concept of quasi-Fermi energy was developed [95]. For example, if a sample is illuminated, quasi-Fermi energy is used for photogenerated electrons, nGe, and quasi-Fermi energy for photogenerated openings, pEf, are used to describe the free energies of electrons and holes in wires and valent bands respectively. However, as El Salvador [126] points out, the use of this statistical concept is called into question in situations relating to the lack of balance between electrons and holes; It is a function of the concentration of holes in the semiconductor surface, which in turn depends on a complex way of illumination intensity, the recombination rate of electronic holes and the speed of charge transfer to the electrolyte [127]. Therefore, the usefulness of the quasi-Fermi concept of uneven energy when applied to photoreactions is questionable. Instead, this article will follow Salvador's recommendation and use the simple concept of the individual energies of photogenerate electrons and holes, and will assume that after termination in larger semiconductor particles, these energies reach levels in the ECB and EVB respectively. The situation with regard to the smaller particles of the Q-state should take into account the photo-induced blue change in the edge of semiconductor absorption; this will be discussed in more detail in Section 9.4.1.2.In the absence of kinetic complications, reactions to interphase transmission that occur during photoelectolytic processes in illuminated semiconductor particles can be systematically represented by reactions (9.5a) and (9.6a):Thus, the two energy requirements for reactions (9.5a) and (9.6a) to be carried out spontaneously are: i.e. the energy of photogenerate electrons must be above the Nernst energy level associated with the Ox/Ox− redox system and the energy of the photogenerate openings must be below the Nernst energy level associated with the red red red system Red+/Redox. Since the semiconductor range of energy is given by:. in the absence of kinetic considerations and their subsequent superpotential, equations (9.12a) and (9.12b) allow us to exhaust the condition for spontaneous photoelectrolysis to occur, the minimum semiconductor strip must be: (9.14)Eg=E(Ox/Ox-)-E(Red+/Red). Figure 9.2 shows the gaps in the bulk range and the band edge positions for a number of semiconductor materials where the semiconductor material is in contact with water electrolytes with pH 1. As indicated by Hagfeldt and Greizell [50], the outer ordinate in Fig. 13. The free energy of the pair of electronic openings is less than the energy of the hole in the tape due to the mobile carriers for charging with significant translation entropy within the conductivity and valent bands.Fig. Position of the edges of the strip on the surface of the range semiconductor elements that are in contact with a water electrolyte of pH 1.It have been shown to affect the relative energies on the edge of the semiconductor valence connections and the energy level of Nernst associated with the redox pair can affect photocatalytic oxidation efficiency. For example, the oxidation efficiency of halogenides in TiO2 follows the sequence I− > Br− > Cl-, codication with the sequence of energy from Nernst E(I2/I−) > E(Br2/Br-) > E(Cl2/Cl−) [128, 129]. In accordance with this result is the observation that the reduction of the pH of the solution, and thus the displacement of the tiO2 valence band to the more positive potentials, leads to an increase in the quantum efficiency of oxidation of khalid.P. Blood, in semiconductor lasers, 2013In quantum wells the level of electron quasi-Fermi is high in the strip due to the high density of HH states, as shown in the central diagram of Fig. 3. this reduces the currents of the radiation and electronic leakage (piki 1.4 and 1.5). At points, p-doping fills the narrowly distributed opening states arising from the high effective mass, reducing the current threshold and its temperature dependence and improving performance modulation (Shekin and Depe, 2002a, 2002b). The analysis was given by Smowton et al., (2007). (see also Crowley et al., 2009; Ozgur, 2009). Charles P. PooleJr, ... Ruslan Windowov, in Superconductivity (Second Edition), 2007The state of the farm level D(EF) can be estimated from q. (1.52): For a typical high temperature superconductor with γ ≈ 0.01 J/mole Cu K we receive (4.13)D(EF)≈4.5 CuV atom states. Deb's temperature can be calculated from the slope of the normal state curve Cn/T-versus-T2, sketched in Fig. 13. Typical values for ΦD are from 200 to 350 K. We use formulas that include freeelectronic approximation. To assess the validity of this approximation, we can use Eq. (1.88), which gives the ratio of γ to magnetic sensitivity φ derived from conductivity electrons, in relation to well-known physical constants.U. Mizuthani, ... E.S. Zijlstra, in Physical Metallurgy (Fifth Edition), 2014 Origin of pseudoplate at farm level can be discussed by two different approaches: one from covalent bonding and another by metal joining (Mizutani, 2010). Let's consider the previous approach, taking into account the alloy of Al-Mn. Here we assume a situation such that both Al and Mn atoms are placed several tenths of a nanometer from each other corresponding to an average atomic distance in the alloy. If the energy levels Al-3p and Mn-3d are close together, the two functions of the atomic waves will overlap and each other. This is called orbital hybridization and leads to bonding and anti-sealing levels as shown in Figure 15a (Mizuthani, 2010). This also applies to the formation of a rigid, i.e. al-Mn alloy phase. Bonding and anti-balaphiding levels will naturally be extended into the corresponding bands, leaving pseudo-lopsing between binding and anti-bonding formed by Mn-3d states mixed with Al-3p states. Figure 15b shows the density of states (DOS) for Al-Mn approximately containing 138 atoms as calculated by Fujiwara in

1989 (Fujiwara, 1989).11 Gaussian curves are roughly delineated in Figure 15b as an eye guide, which is the resulting subgroup Al-3p/Mn-3d binding and anti-bonding. It was found that the level of Fermi falls into the pseudo-gaplops created between subgroups Mn-3D. 15. (a) Formation of bonding and anticonnectivity levels due to orbital hybridisation between adjacent Al-3p and Mn-3d atomic wave functions. (b) Pseudo-padencap formation between connecting and anti-binding subgroups due to orbital hybridizations between Al and Mn atoms in al-Mn approx. 100 000 000 000 000 000 000 000 000 000 000 000 000 000 000 000 000 000 000 000 000 000 000 000 000 000 000 0 (Mizutani, 2010). Gaussian curves are approximately mounted on the sub-range profiles as an eye guide. (For a color version of this figure, the reader refers to the online version of this book.) Al-Mn, mentioned above, is favorably stabilized, since the connecting strip is almost entirely filled with electrons, while the anti-conveyor range remains almost empty. This is the stabilization mechanism due to orbital hybridizations. It is also stressed that orbital hybridisation-induced pseudogasp has nothing to do with the size of the cell of the unit. In other words, the effect of orbital hybridization should not necessarily improve, as the number of atoms in a cell increases. We have an alternative approach to generating pseudo-gapp at farm level. This is due to the interaction FsBz and is approached by the metal adhesive image. Let's consider the traveling electrons, which spread within the periodically arranged ionic potential field. Stationary waves will form when the wavelength of the electric wave coincides with the period of ionic potential. The situation in real space is illustrated in Figure 16a (Mizuthani, 2010). This is called a phenomenon of intervention and is equivalent to the implementation of the Bragg Act. For greater simplicity, consider an electron spreading through a one-dimensional periodical field. Either a stationary wave of sinus or cosine is formed when the wave electron number reaches k = ±π/a, as shown in Figure 16b.12 A close-up view of Figure 16b shows that the electronic energy of the stationary wave of cosine type must be ned relative the value of the free electron, since its density is the highest in the center of the ion, where the potential is the lowest. The opposite is true for the stationary wave of type blue. This is the mechanism for forming an energy gap at the wave number k = ±π/a in the ratio of energy dispersion. 16. (a) Formation of stationary electronic waves as a result of effects on periodically located ion potentials, (b) formation of stationary or sinus waves in a single-dimensional field with periodic ion potential (Mizutani, 2010). At this stage, it is worth mentioning the relationship between the avalanche set defined by the Miller indices (h k l) in real space and the corresponding vector of reciprocal grid G in reciprocal space. To get the simplicity, let's look at a cubic system. The reciprocal vector G, which has the components (h k l) in units 2π/a, is perpendicular to the avalanche set with the same miller indices. In this chapter we often use the vector square of the reciprocal grid | G|2 in units of (2π/a)2. It is then given by the square sum of Miller's indices | G|2=h2+k2+l2 in the case of a cubic system. Figure 17a illustrates the opening of the energy difference of the wave vector obtained by dreaming the vector of the reciprocal grid G100, i.e. k=± | G100|/2=±π/a in a simple cubic grid (Mizutani, 2010). This is certainly due to the interference of electrons with the set of bordering aircraft {100} with | G|2=1. As shown in Figure 17b, a cube with a edge length of 2π/a is constructed in the reciprocal space by perpendicular bisation of six equivalent vectors on a reciprocal grid. This is the Brillouin area of a simple cubic grid through which the energy gap appears. In the case of a simple cubic grid, the distance from Γ to the center X of six planes of a square zone of its Brillouin zone is the same (Figure 17b). 17. (a) Formation of an energy difference at wave number k = ±π/a obtained by k=±π/a by kneming the vector of reciprocal grid G100 into a simple cubic grid (Mizutani, 2010). The level of Fermi is well below the energy difference. (b) The Brillouin area for a simple cubic grid. The surface of Fermi farms with the fermi radius corresponding to the electronic structure in point (a) is schematically drawn. The areas of Brillouin that are in contact with the free sphere of the Farms electron are illustrated in Figure 18 for sc, fcc, gamma brass and 1/1–1–1/1 approx. The Brillouin area for bcc grid containing two atoms per single cell is limited by {110} Rhombin dodecadeedri planes with | G|2=2. The Brillouin area for fcc grid containing four atoms per unit cell consists of eight {111} hexagonal planes with | G|2=3 plus six square planes {200} with | G|2=4, completely limited by 14 planes. The number of Brillouin aircraft in contact The sphere of Farms increases with an increase in the number of atoms per unit of cell. In the case of gamma-brass with 52 atoms per unit of cell, the plane of 12 {330} and 24 {411} zones is located at the same distance from origin to form the 36 atoms of a single unit of cell, 12 {330} and 24 {411} zones are located at the same distance from origin to form a 36-hypocritical polyestra Brilin zone with | G|2=18 as shown in Figure 18c. The Fermi sphere, which touches these plains of the zones, can hold 1,538 electrons per atom. The number of planes of the Brillouin zone additionally increases for 1/1-1/1-1/1, containing 160 atoms per cell unit. As shown in Figure 18d, the Brillouin area is limited by 48 {543}, 24 {710} and 12 {550} planes per zone, resulting in an 84-person Brillouin zone with | G|2=50. The sphere of Fermi, which touches all these plains of the zones, accommodates 2.31 electrons per atom. 18. (a) Plains of the Brillouin zone and entered in the free electric sphere in (a) bcc, (b) fcc, (c) gamma brass and (d) 1/1–1–1/1. In the case of the FCC, the listed Sphere Farms first touches {111} and plains of the zones with | G|2 = 3, since the distance ΓL(= 3/2) is shorter than ΓX(= unity) in units of 2π/a. (e/a)c denotes the atomic ratio electrons obtained for the listed sphere of Fermi. The argument above is made in the free electronic model. In realistic systems, the same arguments are true, except that the energy difference in the plains of the Brillouin zone becomes extreme, so that the surface of the Farms is no longer described by a sphere. The set of granite aircraft interacting with electrons at farm level plays an important role in causing the pseudo-range at farm level. The corresponding vector of reciprocal grid | G|2 is hereinafter called critical. Now one may realize that critical | G|2 value increases as the number of atoms per unit cell increases. Contact on the surface of Fermi with the plains of Brillouin zone takes place simultaneously in each center. Therefore, its effect on DOS will be increased, as the number of plains of the plains of the zone increases. An anomaly in DOS caused by FsBz interactions is called van-Hove singularity. We often encounter such a situation in the IMO that a deep valley is formed in dos, but electronic states remain limited at this minimum. It's called a pseudogap. As underlined in section 2.2.4, its contribution to solid stability will become most effective when formed at farm level. Pseudogas induced by FsBz plays a key role in stabilizing the CMA phase, in which the diffraction spectrum is characterized by a series of bragg peaks. Included are quasi-cords, which also have multiple sharp diffration peaks and more marked pseudo-rough ones better ordered (Mizutani, 2010). Suppose the phenomenon of interference happens at farm level and be strong enough to cause a big pseudogamp there. The situation is now foreseen in such a way that the effective field of Farms with 2kF is in contact with the planes of the Brillouin zone connected to the critical vector of reciprocal grid | G|. This immediately leads to the conditionEcuation 4, claiming the execution of the state of intervention is often referred to as hume-Rothery matching state (Mizutani, 2010). It is important to keep in mind that Eqn 4 is no longer based on the free electronic model. A key point is how to define an effective sphere of Farms and extract the value of 2kF and how to extract the critical vector of a reciprocal grid even for systems containing a large amount of transient metal elements. In the following sections we will introduce an elegant technique based on the first principles of linearized flat wave augmentation calculations (FLAPW) to determine the effective Fermi diameter 2kF and the critical vector of reciprocal grid | G|10000 is involved in Eqn 4 in all intermetal compounds in which chemical disorders and defects are absent and the cell unit is well defined. The compliance condition given by Eqn 4 has been tested for many CMAs and will be discussed as the main topic in the following sections.A few more words may be added in relation to EQN 4. The square with the diameter of Fermi (2kF)2 is expressed in the form (5)2kF)2=[3π(e/a)N]2/3=[3π(e/uc)]2/3,in units of (2π)a)2, where N is the number of atoms per unit of cell and e/uc, product of N and e/a, represents the number of electrons per unit of cell. It is important to recall that (2kF)2 and critical | G|2 in units of (2π/a) 2 and e/uc, as well as an increase in N. This means that these three parameters (2kF)2, critical | G|2 and e/uc can only be defined for crystals, but not for quasicrystal, since the unit cell is infinitely large. However, the parameter e(a) can be defined for quasi-crystals as it is a quantity regardless of N. Note that the e/a value given as the average composition value of the constituents is used not only for crystals, but also for the quaestritis, provided that the e/a values of the constituents are a priori known. Over the past two decades, expressions such as humus roteria stabilization and/or Hume-Rother stabilization have often been used, especially when discussing the stability of quasi-crystals (Mizuthani, 2010; 2005). However, many people use these phrases when a pseudogap is experimentally detected, or theoretically predicted, in the CMA without distinguishing between the two sources: FsBz and orbital hybridizations. Very careful consideration is needed to derive the role of FsBz interactions in the formation of pseudo-pseudogas in the systems in which orbital hybridizations predominate. Our goal in this chapter is to clarify this important issue. Question.